

Eigenoscillations of the differentially rotating Sun: II. Generalization of Laplace's tidal equation

N.S. Dzhililov^{1,2} and J. Staude²

¹ Institute of Terrestrial Magnetism, Ionosphere and Radio Wave Propagation of the Russian Academy of Sciences, Troitsk City, Moscow Region, 142190 Russia; E-Mail: namig@izmiran.rssi.ru

² Astrophysikalisches Institut Potsdam, Sonnenobservatorium Einsteinurm, 14473 Potsdam, Germany; E-Mail: jstaude@aip.de

Received ; accepted

Abstract. The general PDE governing linear, adiabatic, nonradial oscillations in a spherical, differentially and slowly rotating non-magnetic star is derived. This equation describes mainly low-frequency and high-degree g -modes, convective g -modes, and rotational Rossby-like vorticity modes and their mutual interaction for arbitrarily given radial and latitudinal gradients of the rotation rate. Applying to this equation the 'traditional approximation' of geophysics results in a separation into radial- and angular-dependent parts of the physical variables, each of which is described by an ODE. The condition for the applicability of the traditional approximation is discussed. The angular parts of the eigenfunctions are described by Laplace's tidal equation generalized here to take into account differential rotation. From a qualitative analysis of Laplace's tidal equation the sufficient condition for the formation of the dynamic shear latitudinal Kelvin-Helmholtz instability (LKHI) is obtained. A small rotation gradient causes LKHI of prograde waves (seen in the rotating frame), while strong gradients are responsible for retrograde LKHI. The value of the latitudinal rotation gradient has a lower limit, below which LKHI disappears. The LKHI result is applied to real solar helioseismology rotation data. It is shown that the $m = 1$ mode ($m =$ azimuthal wave number) instability can develop. This global instability takes place in the whole envelope of the Sun, including the greatest part of the tachocline, in radial direction and at almost all latitudes in horizontal direction. The exact solutions of Laplace's equation for low frequencies and rigid rotation are obtained. There exists only a retrograde wave spectrum in this ideal case. The modes are subdivided into two branches: fast and slow modes. The long fast waves carry energy opposite to the rotation direction, while the shorter slow-mode group velocity is in the azimuthal plane along the direction of rotation. The eigenfunctions are expressed by Jacobi's polynomials which are polynomials of higher order than the Legendre's for spherical harmonics. The solar 22-year mode spectrum is calculated. It is shown that the slow 22-year modes are concentrated around the equator, while the fast modes are around the poles. The band of latitude where the mode energy is concentrated is narrow, and the spatial place of these band depends on the wave numbers (l, m) .

Key words. hydrodynamics – Sun: activity – Sun: interior – Sun: oscillations – Sun: rotation – Stars: oscillations

1. Introduction

In a recent paper Dzhililov et al. (2001; paper 1) investigated which lowest-frequency eigenoscillations can occur in the real Sun, moreover, which role they play in redistributing angular momentum and causing solar activity. We found that such waves could only be differential rotation Rossby-like vorticity modes. However, the general nonradial pulsation theory adopted from stellar rotation has some difficulties. For slow rotation, when the sphericity of the star is violated not seriously, the degeneracy of the high-frequency spherical p - and g -modes with respect to the azimuthal number m is abandoned by ro-

tation (Unno et al. 1989). Independent of the spherical modes non-rotating toroidal flows (called 'trivial' modes with a zero frequency) become quasi-toroidal with rotation (called r -modes with a nonzero frequency; Ledoux 1951; Papaloizou & Pringle 1978; Provost et al. 1981; Smeyers et al. 1981; Wolff 1998). Although rotation abandons the degeneracy of the modes, it also couples the modes with the same azimuthal order, and this makes the problem more difficult. For the high-frequency modes ($\varepsilon_R = \omega/2\Omega \geq 1$, where ω and Ω are the angular frequencies of oscillations and of stellar rotation, respectively) this difficulty is resolved more or less successfully. For this case the small perturbation rotation theory is applied, in which the eigenfunctions are represented by power series, the an-

gular parts of which are expressed by spherical harmonic functions Y_l^m (Unno et al. 1989). These power series are well truncated, unless $\varepsilon_R < 1$, when the role of Coriolis force is increasing.

Namely the low-frequency instabilities are discovered in most pulsating stars (Cox 1980; Unno et al. 1989). Rotation couples strongly together the high-order g , the convective g , and the r -modes with $\varepsilon_R < 1$ and with the same m , but different l (Lee & Saio 1986). Generally the matrix of the coupling coefficients to be determined is singular (e.g. Townsend 1997). In all papers on the eigenvalue problem of nonradially pulsating stars, there exists a ‘truncation problem’ for the serial eigenfunctions, the angular parts of which are represented by spherical harmonics (e.g. Lee & Saio 1997; Clement 1998).

The governing partial differential equations (PDEs) of the eigenoscillations of rotating stars are complicated from the point of view of the mathematical treatment, even if the motions are adiabatic. This difficulty arises because in spherical geometry an eigenvalue problem with a singular boundary condition has to be solved. These equations are simplified considerably to neglect the tangential components of the angular velocity $\boldsymbol{\Omega}$ in the low-frequency case $\varepsilon_R < 1$ (this means that the motion caused by the Coriolis force is primarily horizontal). This limitation widely used in geophysical hydrodynamics (e.g. Eckart 1960) is called ‘traditional approximation’ and has been used first by Laplace (1778) to study tidal waves (Lindzen & Chapman 1969). Laplace’s equation (or the traditional approximation) for $\varepsilon_R < 1$ is applicable to the stellar case too. The main advantage of this approximation is that it decomposes the initial system of equations into a pair of ordinary differential equations (ODEs) (e.g. Lindzen & Chapman 1969; Berthomieu et al. 1978; Bildsten et al. 1996; Lee & Saio 1997). The angular parts of the eigenfunctions are described by Laplace’s tidal equation. Solving this equation numerically by using a relaxation method, Lee and Saio (1997) first avoided the representation of the solutions by $Y_l^m(\cos\theta)$ functions for the $\Omega = \text{const}$ case, and they had no problem with the truncation of the series.

In the present work for the non-magnetic and non-convective cases we receive one PDE in spherical geometry for the adiabatic pressure oscillations in the differentially rotating star ($\Omega = \Omega(r, \theta)$) with arbitrary spatial gradients of rotation (Sect. 2). This general equation is split into the θ - and r -component ODEs, if the traditional approximation is applied (Sect. 3). The θ -component equation is Laplace’s tidal equation generalized for the differentially rotating case. In Sect. 4 we analyse more qualitatively this equation. We find the general condition for the shear instability due to differential rotation in latitude. We find that the smallest rotation gradient is responsible for the prograde (seen in the rotating frame) vorticity wave instability, while a stronger gradient causes the retrograde wave instability. For solar data (small rotation gradients) the $m = 1$ prograde mode instability is possible (Sect. 4.4). The possible existence of such a global horizontal shear instability on the Sun has been investigated by Watson

(1981) and Gilman & Fox (1997), that of shear and other dynamic instabilities and of thermal-type instabilities in stars as well by Knobloch & Spruit (1982) and others. Laplace’s tidal equation for low frequencies in the rigid-rotation case is investigated in detail in Sect. 5. It is shown that the eigenfunctions are defined by Jacobi’s polynomials which are of higher order than the Legendre’s.

2. Basic equations

The fluid motion in a self-gravitating star, neglecting a magnetic field and viscosity, may be described in an inertial frame by the hydrodynamic equations. These equations in conventional definition are written as

$$\frac{\partial \rho}{\partial t} + \nabla \cdot (\rho \mathbf{V}) = 0, \quad (1)$$

$$\rho \left(\frac{\partial}{\partial t} + \mathbf{V} \cdot \nabla \right) \mathbf{V} = -\nabla p - \rho \nabla \Phi, \quad (2)$$

$$\rho T \left(\frac{\partial}{\partial t} + \mathbf{V} \cdot \nabla \right) s = \rho \varepsilon_N - \nabla \cdot \mathbf{F}, \quad (3)$$

$$\nabla^2 \Phi = 4\pi G \rho. \quad (4)$$

2.1. Equilibrium state

We suppose that the equilibrium state (variables with zero indices) of the star is stationary and that its differential rotation is axially symmetric:

$$\mathbf{V}_0(r, \theta) = \boldsymbol{\Omega} \times \mathbf{r} = \Omega r \sin\theta \mathbf{e}_\phi, \quad (5)$$

where $\boldsymbol{\Omega}(r, \theta) = \Omega_r \mathbf{e}_r + \Omega_\theta \mathbf{e}_\theta$, with the components $\Omega_r = \Omega \cos\theta$, $\Omega_\theta = -\Omega \sin\theta$, and $\Omega_\phi \equiv 0$, is the stellar angular velocity of rotation described in spherical polar coordinates, (r, θ, ϕ) . Here \mathbf{e}_i with $i = r, \theta, \phi$ are the unit vectors. We will not include convective motion and meridional flows into the initial steady state. In that case we may obtain, in particular from the Eq.(2) of motion, the hydrostatic equilibrium relation

$$-\frac{\nabla p_0}{\rho_0} = \nabla \left(\Phi_0 - \frac{1}{2} |\boldsymbol{\Omega} \times \mathbf{r}|^2 \right) + \Omega r^2 \sin^2\theta \nabla \Omega = \tilde{\mathbf{g}}. \quad (6)$$

It follows that the effective gravity $\tilde{\mathbf{g}}$ cannot be a potential field if differential rotation $\nabla \Omega \neq 0$ is present. This is important for rapidly rotating stars where the configuration is deformed by the centrifugal force as well as by differential rotation. For slowly rotating stars (the Sun as well) we may assume that the initial state is only marginally disturbed by rotation and $\tilde{\mathbf{g}} \approx \mathbf{g} = \nabla \Phi_0$ can be applied. That is, non-sphericity is not essential for the generation of waves (Unno et al. 1989).

2.2. Equations of oscillation

Small amplitude deviations from the basic state of the star may be investigated by linearizing Eqs. (1–4). For

Eulerian perturbations (variables with a prime) the equation of motion becomes (Unno et al. 1989)

$$\begin{aligned} e_i \frac{\partial}{\partial t'} V_i + 2\boldsymbol{\Omega} \times \mathbf{V} + e_\phi r \sin\theta (\mathbf{V} \cdot \nabla\Omega) = \\ = \frac{\nabla p_0}{\rho_0} \frac{\rho'}{\rho_0} - \frac{1}{\rho_0} \nabla p' - \nabla\Phi'. \end{aligned} \quad (7)$$

Here the operator

$$\frac{\partial}{\partial t'} = \frac{\partial}{\partial t} + \Omega \frac{\partial}{\partial\phi} \quad (8)$$

represents the temporal derivative referring to a local frame rotating with an angular velocity $\Omega = \Omega(r, \theta)$. For low-frequency waves Saio (1982) has shown numerically in detail, that the Cowling approximation is good enough in most cases. Thus we will neglect perturbation of the gravitational potential in Eq. (7), $\Phi' = 0$. We are interested in very slow motions such that $v_{\text{ph}} \ll c_s$, where v_{ph} is the phase velocity of the waves and c_s is the sound speed. Then the incompressible fluid motion limit, $c_s^2 \rightarrow \infty$ (it is within the adiabatic approximation) may be applied, and instead of the Eq. (1) of mass conservation we use

$$\nabla \cdot \mathbf{V} = \frac{1}{r^2} \frac{\partial(r^2 V_r)}{\partial r} + \frac{1}{r \sin\theta} \frac{\partial(V_\theta \sin\theta)}{\partial\theta} + \frac{1}{r \sin\theta} \frac{\partial V_\phi}{\partial\phi} = 0. \quad (9)$$

We have shown in Paper 1, that nonadiabatic effects are of great importance for the dynamics of low-frequency rotation modes. However, here we shall restrict ourselves to the adiabatic case only because the mathematical treatment of wave equations in spherical geometry is rather difficult. For adiabatic waves we receive from Eq. (3)

$$\frac{\partial\rho'}{\partial t'} - \rho_0 \frac{N^2}{g} V_r = \frac{1}{c_s^2} \frac{\partial p'}{\partial t'}, \quad (10)$$

where the squared Brunt-Väisälä frequency

$$N^2 = g \left(\frac{1}{\Gamma_1} \frac{1}{p_0} \frac{dp_0}{dr} - \frac{1}{\rho_0} \frac{d\rho_0}{dr} \right) \quad (11)$$

is written for the slow rotation case where $\tilde{g} \approx g$. For rapid rotation $N^2 = N^2(r, \theta)$ and g should be changed here to \tilde{g} . In the incompressible limit ($c_s^2 \rightarrow \infty$) Eq. (10) reads

$$\frac{\partial\rho'}{\partial t'} = \rho_0 \frac{N^2}{g} V_r. \quad (12)$$

Thus we have a complete set of Eqs. (7, 9, 12) to describe adiabatic, low-frequency, non-radial oscillations in a differentially rotating star. For our axisymmetric stationary initial state we may represent all the perturbed variables \mathbf{V} , p' , and ρ' in the inertial frame as

$$\mathbf{V}(r, \theta, \phi; t) \implies \mathbf{V}(r, \theta) e^{i(m\phi - \omega_0 t)}. \quad (13)$$

Considering $\partial/\partial t' = -i\omega$ and $\partial/\partial\phi = im$ we find from Eq. (8) the relation between the frequencies in the inertial and rotating frames

$$\omega = \omega_0 - m\Omega(r, \theta), \quad (14)$$

from where we get $\nabla\omega = -m\nabla\Omega$. If we separate the variable part of the rotation frequency, $\Omega(r, \theta) = \Omega_\odot + \tilde{\Omega}(r, \theta)$, then $\omega = \omega_0 - m\Omega_\odot - m\tilde{\Omega} = \omega_\odot - m\tilde{\Omega} = \omega_\odot - k_\phi v_{\text{ph}}$ (k_ϕ and v_{ph} are the local azimuthal wave number and the phase velocity, respectively). We will study the case $\tilde{\Omega} \ll \Omega_\odot$. From now $\Omega \approx \Omega_\odot$ and $\nabla\Omega = \nabla\tilde{\Omega} \neq 0$ will be used. Low frequencies seen in the rotating frame mean that we are close to the resonant frequencies in the inertial frame ($\omega_\odot \approx k_\phi v_{\text{ph}}$).

Now excluding ρ' from Eq. (7) by using Eq. (12), taking the projection of this equation onto the rotation axis $\boldsymbol{\Omega}$ and two tangential components as well, and adding Eq. (9) we get

$$\begin{aligned} \left(1 - \frac{N^2}{\omega^2}\right) V_r \cos\theta - j V_\theta \sin\theta = \\ = \frac{1}{\rho_0 i\omega} \left(\cos\theta \frac{\partial}{\partial r} - j \frac{\sin\theta}{r} \frac{\partial}{\partial\theta} \right) p', \end{aligned} \quad (15)$$

$$V_\theta + \frac{2\Omega \cos\theta}{i\omega} V_\phi = \frac{1}{r\rho_0 i\omega} \frac{\partial p'}{\partial\theta}, \quad (16)$$

$$\begin{aligned} -i\omega V_\phi + j \sin\theta \left(2\Omega + r \frac{\partial\Omega}{\partial r}\right) V_r + \\ + \left(2\Omega \cos\theta + \sin\theta \frac{\partial\Omega}{\partial\theta}\right) V_\theta = -\frac{im}{r\rho_0 \sin\theta} p', \end{aligned} \quad (17)$$

$$imV_\phi + \frac{\sin\theta}{r} \frac{\partial}{\partial r}(r^2 V_r) + \frac{\partial}{\partial\theta}(\sin\theta V_\theta) = 0. \quad (18)$$

Here we have introduced the special parameter j to switch to the traditional approximation ($\Omega_\theta = 0$, $\Omega_r \neq 0$). In the general case $j \equiv 1$, and for switching to the traditional approximation we put $j = 0$. Further we will obtain one additional equation for p' .

Let $\mu = \sin\theta$ be a new independent variable and

$$\begin{aligned} \varepsilon_R = \frac{\omega}{2\Omega}, \quad \beta_r = \frac{r}{2\Omega} \frac{\partial\Omega}{\partial r}, \quad \beta_\mu = \frac{\mu}{2\Omega} \frac{\partial\Omega}{\partial\mu}, \\ \alpha = \varepsilon_R^2 - (1 - \mu^2)(1 + \beta_\mu), \\ a_1 = \frac{1 + \beta_r}{\varepsilon_R}, \quad a_2 = \frac{1 + \beta_\mu}{\varepsilon_R}, \quad a_3 = \frac{\alpha}{\varepsilon_R^2}, \\ a_4 = \mu^2 \frac{1 + \beta_r}{\alpha}, \quad a_5 = \frac{m}{\varepsilon_R}(1 + \beta_\mu) - 1. \end{aligned} \quad (19)$$

ε_R is the Rossby number; we are interested in $\varepsilon_R \leq 1$. Using

$$iV_\phi = ja_1\mu V_r + a_2 V_\theta \cos\theta - \frac{m}{\rho_0 i\omega} \frac{p'}{r\mu} \quad (20)$$

we get three equations from the Eqs. (15–18) for V_r , V_θ , and p' . From those V_θ is excluded by

$$\frac{V_\theta}{\cos\theta} = ja_4 \tilde{V}_r - \frac{1}{a_3} \left(a_5 - \mu \frac{\partial}{\partial\mu} \right) \tilde{P}, \quad (21)$$

where

$$p' = \mu r \rho_0 i\omega \tilde{P}, \quad V_r = \mu \tilde{V}_r, \quad (22)$$

and we get two equations for \tilde{V}_r and \tilde{P} :

$$\begin{aligned} & \left(1 - \frac{N^2}{\omega^2} - ja_4\right) \tilde{V}_r = \\ & = \left[b_1 + r \frac{\partial}{\partial r} - ja_6 - j \left(1 - \frac{1}{a_3}\right) \mu \frac{\partial}{\partial \mu}\right] \tilde{P}, \end{aligned} \quad (23)$$

$$\left[2 + r \frac{\partial}{\partial r} + j \left(a_8 + a_9 \mu \frac{\partial}{\partial \mu}\right)\right] \tilde{V}_r = \check{A}(\mu) \tilde{P}, \quad (24)$$

$$\check{A}(\mu) = \frac{1}{\mu^2} \left[a_7 + (1 - \mu^2) \mu \frac{\partial}{\partial \mu} \right] \frac{1}{a_3} \left(a_5 - \mu \frac{\partial}{\partial \mu} \right) + \frac{m^2}{\mu^2}.$$

Here the dimensionless coefficients are defined as

$$\begin{aligned} a_6 &= \frac{1}{\alpha} \left[m \varepsilon_R + (1 - \mu^2)(1 + \beta_\mu) \left(\frac{m}{\varepsilon_R} \beta_\mu - 1 \right) \right], \\ a_7 &= \frac{m}{\varepsilon_R} (1 + \beta_\mu)(1 - \mu^2) + 1 - 2\mu^2, \\ a_8 &= \frac{a_8^*}{\alpha^2}; \quad a_9 = \frac{1}{\alpha} (1 - \mu^2)(1 + \beta_r), \\ a_8^* &= (1 + \beta_r) \left[\alpha(3 - 4\mu^2 + m \varepsilon_R) - \right. \\ & \quad \left. - (1 - \mu^2) \check{\delta}_\mu \alpha \right] - 2\alpha(1 - \mu^2) \beta_r \beta_\mu, \\ b_1 &= 1 + \varkappa_\rho - \frac{m}{\varepsilon_R} \beta_r, \quad \varkappa_\rho = \frac{r}{\rho_0} \frac{d\rho_0}{dr}. \end{aligned} \quad (25)$$

Deriving these equations the second derivatives $\Omega''(\theta)$ and $\Omega''(r)$ have been omitted as very small quantities. Eq. (23) allows to obtain one equation for p' :

$$\left[\psi_1 \check{\delta}_r^2 + \psi_2 \check{\delta}_\mu^2 + \psi_3 \check{\delta}_r + \psi_4 \check{\delta}_\mu + \psi_5 \check{\delta}_r \check{\delta}_\mu + \psi_6 \right] \tilde{P} = 0. \quad (26)$$

This is the main singular PDE for nonradial rotation-gravity waves in a differentially rotating star. The coefficients ψ_{1-6} of Eq. (26) are rather complicated, we present them in Appendix A. The operators are defined as

$$\check{\delta}_r = r \frac{\partial}{\partial r}, \quad \check{\delta}_\mu = \mu \frac{\partial}{\partial \mu}, \quad \text{and} \quad \check{\delta}_r^2 = \check{\delta}_r \check{\delta}_r. \quad (27)$$

First we will study this equation in different simplified approximations. The most popular case is the traditional approximation.

3. The ‘traditional approximation’: $j \equiv 0$

Strictly speaking, the condition $j = 0$ in Eq. (26) is not applicable in two points: (1) at $\omega^2 = N^2(r)$, that is in the turning points in radial direction; (2) at $\alpha = 0$ or $\varepsilon_R^2 \approx \cos^2 \theta$, that is in the latitudinal turning point. The last one is more important, because the traditional approximation filters out such important and interesting phenomena as the trapping of Rossby-like waves around the equator. In geophysics this phenomenon is investigated separately (Pedlosky 1982; Gill 1982). The applicability of the traditional approximation for rigid rotation has been checked by numerical modelling as well as by experimental verification. For minor differential rotation of the star

(small β_r and β_μ) these examinations are also valid. Thus for $j = 0$ Eq. (26) becomes:

$$\begin{aligned} & \frac{\varepsilon_R}{\alpha^2 \mu^2} \left[\alpha \varepsilon_R (1 - \mu^2) \mu^2 \frac{\partial^2}{\partial \mu^2} + q_3 \mu \frac{\partial}{\partial \mu} + q_4 \right] p' = \\ & = -\frac{1}{\psi} \left(r^2 \frac{\partial^2}{\partial r^2} + b_4 r \frac{\partial}{\partial r} + b_5 \right) p' \end{aligned} \quad (28)$$

with the parameters

$$\begin{aligned} q_1 &= 2 - \mu^2 - \varepsilon_R^2 \frac{2 - 3\mu^2}{1 - \mu^2} + \\ & \quad + \beta_\mu \left[2\mu^2 - 1 - 2(1 - \mu^2)(1 + \beta_\mu)(m/\varepsilon_R + 1) \right], \\ q_2 &= h_0 + h_1 \beta_\mu + h_2 \beta_\mu^2, \\ h_0 &= \varepsilon_R (m^2 - 1)(\varepsilon_R^2 + \mu^2 - 1) - \\ & \quad - \mu^2 [m(1 - \mu^2) + \varepsilon_R^2 (m - 2\varepsilon_R)], \\ h_1 &= (1 - \mu^2) \left[-2m\mu^2 + \varepsilon_R (m^2 - 4 + 5\mu^2) + \right. \\ & \quad \left. + 4m\varepsilon_R^2 \right] - m\varepsilon_R^2, \\ h_2 &= (1 - \mu^2)^2 (3m - 2\varepsilon_R + 2m\beta_\mu) - \\ & \quad - (1 - \mu^2)m(1 - 2m\varepsilon_R), \\ b_2 &= 3 + \varkappa_\rho - \beta_r \frac{m}{\varepsilon_R} - \frac{\check{\delta}_r \psi}{\psi}, \\ b_3 &= 2 + 3\varkappa_\rho - \beta_r \frac{m}{\varepsilon_R} \left(3 + \beta_r \frac{m}{\varepsilon_R} \right) - \\ & \quad - \left(1 + \varkappa_\rho - \beta_r \frac{m}{\varepsilon_R} \right) \frac{\check{\delta}_r \psi}{\psi}, \\ \psi &= 1 - \frac{N^2}{\omega^2}, \quad \check{\delta}_r \psi = -2 \frac{N^2}{\omega^2} \frac{m}{\varepsilon_R} \beta_r - \frac{r}{\omega^2} \frac{dN^2}{dr} \end{aligned} \quad (29)$$

$$\begin{aligned} q_3 &= \varepsilon_R (1 - \mu^2) [\alpha(1 - 2a_0) - q_1], \quad a_0 = 1 - \beta_\mu \frac{m}{\varepsilon_R}, \\ q_4 &= \varepsilon_R (1 - \mu^2) [\alpha(a_0^2 - \check{\delta}_\mu a_0) + a_0 q_1] - q_2, \\ \check{\delta}_\mu a_0 &= -\beta_\mu \frac{m}{\varepsilon_R} \left(1 + \beta_\mu \frac{m}{\varepsilon_R} \right), \\ b_4 &= 1 - 2b_1 + b_2, \quad \check{\delta}_r b_1 = \varkappa_\rho - \beta_r \frac{m}{\varepsilon_R} \left(1 + \beta_r \frac{m}{\varepsilon_R} \right), \\ b_5 &= b_1^2 - \check{\delta}_r b_1 - b_1 b_2 + b_3. \end{aligned}$$

Remembering that $\tilde{\Omega}(r, \theta) \ll \Omega_\odot$, the left-hand side of Eq. (28) is a function of $\mu = \sin \theta$, while the right-hand side is a function of r only. In that way we may separate the variables

$$p'(r, \mu) = \Theta(\mu) Q(r). \quad (30)$$

Now putting Eq. (30) into (28) we receive the ‘ θ ’- and ‘ r ’-equations:

$$\left[\alpha \varepsilon_R (1 - \mu^2) \mu^2 \frac{d^2}{d\mu^2} + q_3 \mu \frac{d}{d\mu} + q_4 + \Lambda \frac{\alpha^2 \mu^2}{\varepsilon_R} \right] \Theta(\mu) = 0, \quad (31)$$

$$\left(r^2 \frac{d^2}{dr^2} + b_4 r \frac{d}{dr} + b_5 - \Lambda \psi \right) Q(r) = 0. \quad (32)$$

These two equations are connected to each other by two common spectral parameters: ω – the oscillation frequency

and Λ – the separation parameter. Both must be searched for as a solution of the boundary value problem. So far the logarithmic gradients of the rotation rate are arbitrary functions, $\beta_\mu = \beta_\mu(\mu)$, $\beta_r = \beta_r(r)$.

4. Generalized Laplace's tidal equation

Eq. (31) is the generalized Laplace equation if differential rotation is present, $\beta_\mu \neq 0$. For rigid rotation, $\beta_\mu = 0$, Eq. (31) becomes the standard Laplace equation:

$$-\frac{1}{\varepsilon_R^2 - \mu_*^2} \left(\frac{m^2}{1 - \mu_*^2} - \frac{m}{\varepsilon_R} \frac{\varepsilon_R^2 + \mu_*^2}{\varepsilon_R^2 - \mu_*^2} \right) + \frac{\Lambda}{\varepsilon_R^2} \Big] \Theta = 0, \quad (33)$$

where $\mu_* = \cos \theta$. A peculiarity of this equation is the presence of three singular points: at the pole, at the equator, and between both if $\varepsilon_R^2 \leq 1$ (our case). Therefore it is hard to solve such an equation analytically or numerically to find the eigenvalues. Since the time of Laplace in geophysics investigations were focused on almost two-dimensional (horizontal) motions in strongly stratified fluids with $V_r \approx 0$. In this situation the r -component Eq. (32) does not appear, and one is looking for the eigenvalues Λ in Laplace's Eq. (33) for a given ε_R (it is expressed through the thickness of the fluid layer, e.g., in a shallow water-wave system). For the special cases and for the general case too, when the eigenfunctions are expressed through the Hough functions (essentially these are the same infinite series of Y_l^m harmonics) references could be found in a paper by Lindzen & Chapman (1969).

In astrophysics the r -component Eq. (32) appears, and two equations must be solved together to find both spectral parameters. In the rigid-rotation case Lee and Saio (1997) looked for Λ numerically in an approach similar to that in geophysics, fixing ε_R in Eq. (33). We offer here another approach, where we will find Λ from the r -equation for a given $\varepsilon_R \leq 1$.

It is convenient to introduce into Eq. (31) the new variable $x = \mu^2 = \sin^2 \theta$:

$$4(1 + \beta_\mu)(1 - x)(x - a)x^2 \frac{d^2 \Theta}{dx^2} - A_1 2x \frac{d\Theta}{dx} + A_2 \Theta = 0, \quad (34)$$

where

$$A_1 = (1 - x)[2 - x - 3\varepsilon_R^2 + \beta_\mu(4x - 3 - 2m\varepsilon_R)] - 2\beta_\mu^2(1 - x)^2 + \varepsilon_R^2, \quad (35)$$

$$A_2 = (1 - x)[m^2(1 - \beta_\mu) + \frac{m}{\varepsilon_R}x + \beta_\mu \frac{m}{\varepsilon_R}(4x - 3 - 2\varepsilon_R^2)] - m\varepsilon_R(1 - x) + m\varepsilon_R(1 - m\varepsilon_R) + \frac{\Lambda}{\varepsilon_R^2}x(x - a)^2(1 + \beta_\mu)^2,$$

$$a = 1 - \frac{\varepsilon_R^2}{1 + \beta_\mu}. \quad (36)$$

This equation determines the tangential structure of the eigenfunctions, while Eq. (32) is responsible for the radial behavior. A detailed investigation of Eq. (32) is not

included in this work. A similar equation for a realistically stratified model of the Sun has been investigated by Oraevsky & Dzhililov (1997). We remind that the radial structure of the eigenfunctions depends on the sign of Λ (either radiative or convective modes). Now we can already estimate an approximate value of Λ :

$$\frac{\Lambda}{\varepsilon_R^2} \sim \frac{n^2 \pi^2}{N_m^2 \varepsilon_R^2 / \omega^2} = \frac{n^2 \pi^2}{N_m^2 / 4\Omega^2} \sim n^2 \times 10^{-6}, \quad (37)$$

where n is the radial harmonic number, N_m is mean value of the Brunt-Väisälä frequency in the radiative interior or in the convection zone, and $N_m/2\Omega$ is the Prandtl number. An estimate of Eq. (37) is done for a solar model, but we think similar values of the Prandtl number are valid for most other stars too. Thus we can omit from A_2 in Eq. (35) the last term, if the radial number n is not too large.

4.1. Fluid velocities

From Eqs. (20, 21, 23) we can derive in the traditional approximation the following formulae for the components of the fluid velocity:

$$V_r = \frac{1}{\rho_0 i \omega \psi} \frac{\partial p'}{\partial r}, \quad (38)$$

$$V_\theta = \frac{\pm 1}{r \rho_0 i \omega} \frac{\varepsilon_R^2}{1 + \beta_\mu} \frac{1 - x}{a - x} \frac{1}{\sqrt{x(1 - x)}} \left(\frac{m}{\varepsilon_R} - 2x \frac{\partial}{\partial x} \right) p', \quad (39)$$

$$V_\phi = \frac{1}{r \rho_0 \omega} \frac{1}{\sqrt{x}} \left[\frac{1 - x}{a - x} \left(2\varepsilon_R x \frac{\partial}{\partial x} - m \right) + m \right] p'. \quad (40)$$

Here the different signs \pm of V_θ correspond to the northern and southern hemispheres, so that $\cos \theta = \pm \sqrt{1 - x}$. Our further aim is to find such solutions for $p' = \Theta(x)Q(r)$ that all the components of the velocity remain limited at the pole ($x = 0$), at the equator ($x = 1$), and in both turning points, where $x = a$ and $\psi(r) = 0$.

4.2. Heun's equation

Now we will impose a restriction to $2\beta_\mu = \partial(\ln \Omega)/\partial(\ln \mu) \approx \text{const}$, the logarithmic latitudinal gradient of the rotation frequency. We might take the linear dependence $\beta \sim x$, but for such a profile the structure of the solutions is not changed qualitatively. Let us introduce the new dependent variable

$$\Theta = x^\sigma Y(x), \quad (41)$$

where

$$2\sigma = \beta_\mu S_1 \pm \sqrt{\beta_\mu^2 S_1^2 - S_2} = 2\sigma_{1,2}, \quad (42)$$

$$S_1 = \frac{5 + 2m\varepsilon_R + 2\beta_\mu}{2(1 + \beta_\mu - \varepsilon_R^2)},$$

$$S_2 = \frac{\beta_\mu \frac{m}{\varepsilon_R} (3 + 2\varepsilon_R^2) - m^2(1 - \beta_\mu - \varepsilon_R^2)}{1 + \beta_\mu - \varepsilon_R^2}.$$

Then for $Y(x)$ we get a new equation from Eq. (34)

$$x(1-x)(x-a)Y'' + \frac{1}{2} \left[4\sigma(1-x)(x-a) - \frac{A_1}{1+\beta_\mu} \right] Y' - [(x-1)\nu_0 + \varepsilon_R \nu_1] Y = 0, \quad (43)$$

with

$$\begin{aligned} \nu_0 &= \frac{1+4\beta_\mu}{4(1+\beta_\mu)} \left(\frac{m}{\varepsilon_R} - 2\sigma \right) + \sigma\beta_\mu(S_1-1) - \frac{S_2}{4}, \\ \nu_1 &= \frac{m(m\varepsilon_R-1) + 2\sigma\varepsilon_R}{4(1+\beta_\mu)}. \end{aligned} \quad (44)$$

Eq.(43) is Heun's equation (Heun 1889) in standard form

$$x(x-1)(x-a)Y'' + [\gamma(x-1)(x-a) + \delta x(x-a) + \varepsilon x(x-1)]Y' + \tilde{\alpha}\tilde{\beta}(x-h)Y = 0. \quad (45)$$

The Riemannian scheme for this equation is

$$p \left\{ \begin{array}{cccc} 0 & 1 & a & \infty \\ 0 & 0 & 0 & \tilde{\alpha} \\ 1-\gamma & 1-\delta & 1-\varepsilon & \tilde{\beta} \end{array} \right\},$$

where the exponents are connected by Riemann's relation

$$\tilde{\alpha} + \tilde{\beta} - \gamma - \delta - \varepsilon + 1 = 0.$$

In the Riemann scheme the first row defines the singular points of Heun's equation, while the corresponding exponents are placed in the second and third rows. These exponents are

$$1-\gamma = \beta_\mu S_1 - 2\sigma, \quad 1-\delta = \frac{1}{2}, \quad (46)$$

$$\begin{aligned} 1-\varepsilon &= 2 + \beta_\mu \left(1 - S_1 + \frac{3/2}{1+\beta_\mu} \right), \\ 2\tilde{\alpha} &= S+q, \quad 2\tilde{\beta} = S-q, \quad q = \sqrt{S^2 - 4\nu_0}, \\ h &= 1 - \varepsilon_R \frac{\nu_1}{\nu_0}, \quad S = 2\sigma - 2 - \beta_\mu + \frac{3/2}{1+\beta_\mu}. \end{aligned} \quad (47)$$

Note that the second exponent at $x = a$ is $(1-\varepsilon) \rightarrow 2$ if $\varepsilon_R \rightarrow 0$ or if $\beta_\mu \rightarrow 0$. If $\beta_\mu \rightarrow \infty$ then $(1-\varepsilon) \rightarrow 7/2$. That means, the second independent solution of Eq. (45) with the exponent $(1-\varepsilon)$ is regular at the singular point $x = a$ for all variables, which follows from Eqs. (38–40). The exponent $(1-\delta) = 1/2$ also provides limited V_θ and V_ϕ at the equator ($x = 1$). The singularity $x = \infty$ in the Riemann scheme does not occur in our task. The situation is more complicated around the pole $x = 0$ with the exponent $(1-\gamma)$. Let us consider this point in detail.

4.3. Condition for the latitudinal Kelvin-Helmholtz instability

If we put the solutions with the exponents 0 and $(1-\gamma)$ into Eq. (41) we get $p' \sim \Theta \sim x^{\sigma_{1,2}}$. Then $V_{\theta,\phi} \sim x^{(2\sigma-1)/2}$ means that for the regularity of the solutions at the pole the condition $Re(2\sigma) \geq 1$ must be obeyed. On the other hand, an instability is possible when the eigenfrequencies

are complex, that means complex σ . For the latter it follows from Eq. (42), that the necessary condition is $S_2 > 0$. It is clear that the axially-symmetric mode with $m = 0$ is excluded. For lower values of the rotation gradient $|\beta_\mu| < 1$ the necessary condition $S_2 > 0$ demands for the prograde waves ($m\varepsilon_R > 0$) the condition $\beta_\mu > 0$, which is more realistic for stellar situations (equatorward spinning up at the surface with radius r). Rayleigh's necessary condition for instability (Rayleigh 1880; Watson 1981) says that the function $Rl = \partial^2(\Omega \sin^2 \theta) / \partial \cos^2 \theta$ (gradient of vorticity) must change its sign in the flow. Rewriting this function in our definitions we get that

$$Rl = \frac{2\Omega}{\mu^2} [3\beta_\mu - \mu^2(1+4\beta_\mu)] \quad (48)$$

may change its sign if $\beta_\mu > 0$. There are instability possibilities for negative β_μ which are not considered in this work. However, all formulas are valid for this case too.

The sufficient condition for instability is obtained from Eq. (42) and reads $\beta_\mu^2 S_1^2 < S_2$. The regularity condition at the pole $\beta_\mu S_1 \geq 1$ can be rewritten as

$$\frac{\varepsilon_R}{m} \leq \frac{\beta_\mu \varepsilon_R^2}{1 - \varepsilon_R^2 - \beta_\mu(\beta_\mu + 3/2)} = \chi_3. \quad (49)$$

By this condition the phase space $\{\varepsilon_R/m, \varepsilon_R^2\}$ is divided into three parts, depending on the values of β_μ . For $0 \leq \beta_\mu < 1/2$ we have the following situation: if $\varepsilon_R^2 < 1 - \beta_\mu(\beta_\mu + 3/2)$ the condition Eq. (49) is fulfilled for prograde waves $\varepsilon_R/m \geq 0$ (region **I**); in the opposite case when $\varepsilon_R^2 > 1 - \beta_\mu(\beta_\mu + 3/2)$ the condition (49) is fulfilled for retrograde waves with $\varepsilon_R/m < -1/2$ (region **III**); for $\varepsilon_R^2 = 1 - \beta_\mu(\beta_\mu + 3/2)$ these regions are separated by the asymptote $\chi_3 = \infty$.

For $\beta_\mu > 1/2$ (strong gradients) the condition Eq. (49) is met only for retrograde waves in the range $-1/2 < \varepsilon_R/m \leq 0$ (region **II**). For $\beta_\mu = 1/2$ we get for any ε_R that $\chi_3 = -1/2$. This is the line between the regions **II** and **III**. All three regions are shown in Fig. 1a. It is seen that the regularity condition is working for $|m| \geq 1$ and $|\varepsilon_R| \leq 1$ if $\beta_\mu \neq 0$. For very small β_μ only modes with large m are possible. The smallest $m \gtrsim 1$ modes may appear in the limit $\varepsilon_R \approx 1$. These conclusions are correct only if the instability occurs.

Now let us consider the second condition, the complex frequency condition $\beta_\mu^2 S_1^2 < S_2$. This inequality may be rewritten as

$$\chi_2 < \frac{\varepsilon_R}{m} < \chi_1, \quad (50)$$

$$\begin{aligned} \chi_{1,2} &= \frac{2}{\beta_\mu(5+2\beta_\mu)^2} \left[b_* \pm \sqrt{b_*^2 - a_* \varepsilon_R^2 (5+2\beta_\mu)^2} \right], \\ a_* &= (1 - \varepsilon_R^2)(1 - \varepsilon_R^2 - \beta_\mu^2), \\ b_* &= (3 + 2\varepsilon_R^2)(1 - \varepsilon_R^2 + \beta_\mu) - \varepsilon_R^2 \beta_\mu (5 + 2\beta_\mu). \end{aligned}$$

In the limiting cases we have

$$\chi_1 \approx \frac{12(1+\beta_\mu)}{\beta_\mu(5+2\beta_\mu)^2}, \quad \chi_2 \approx 0 \quad \text{for } \varepsilon_R \rightarrow 0, \quad (51)$$

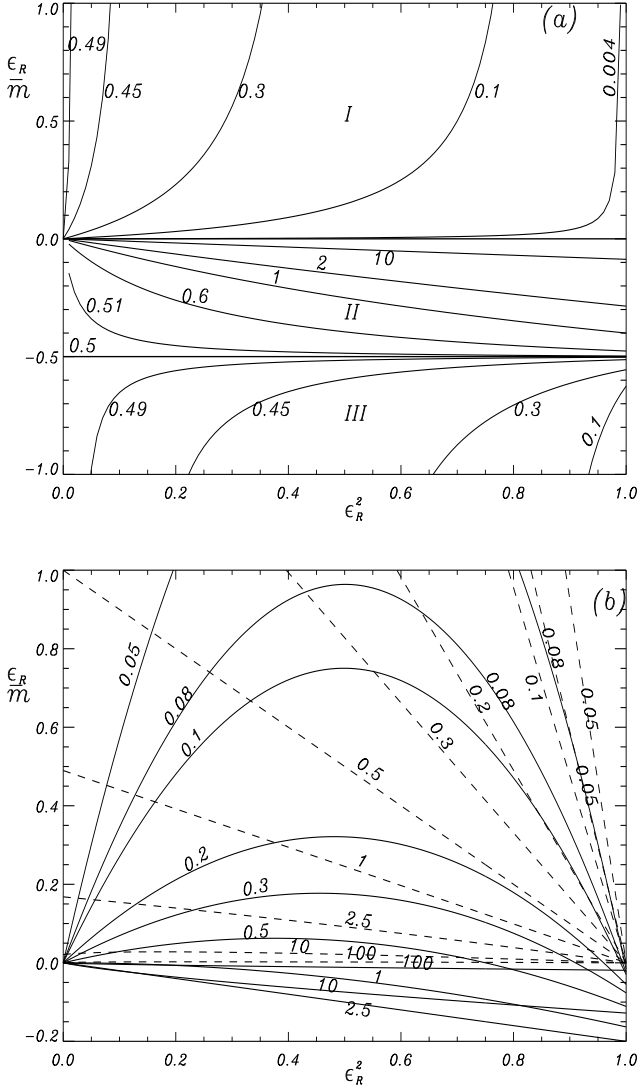


Fig. 1. The domains of validity of the solution regularity and of the instability conditions in the phase space $\{\epsilon_R/m, \epsilon_R^2\}$ for given values of the rotation gradient β_μ . (a) shows the values $\epsilon_R/m = \chi_3$, Eq. (49). In the area $\epsilon_R/m \leq \chi_3$ the solutions are limited at the pole. (b) shows the behavior of χ_1 (dashes) and χ_2 (solid). Between the solid and dashed lines with the same labels (values of β_μ) LKHI is possible.

$$\chi_1 \approx 0, \quad \chi_2 \approx -\frac{8\beta_\mu}{(5 + 2\beta_\mu)^2} \quad \text{for } \epsilon_R \rightarrow 1. \quad (52)$$

In Fig. 1b we plot for $|m| \geq 1$ and $\epsilon_R \leq 1$ the curves χ_1 and χ_2 versus ϵ_R^2 for a wide range of β_μ . A comparison of Figs. 1a and 1b shows that in the region III with $\epsilon_R/m < -1/2$ LKHI will never appear. In the region I LKHI is possible for prograde waves, if $\beta_\mu < 1/2$ and $\epsilon_R^2 < 1 - \beta_\mu(\beta_\mu + 3/2)$. With decreasing β_μ the solid and dashed curves for the same β_μ are close to $\epsilon_R \approx 1$. For retrograde waves LKHI is possible for strong gradients of $\beta_\mu > 1/2$ only in the range $-0.2 \leq \epsilon_R/m < 0$. Here $(\chi_2)_{\min} = -0.2$

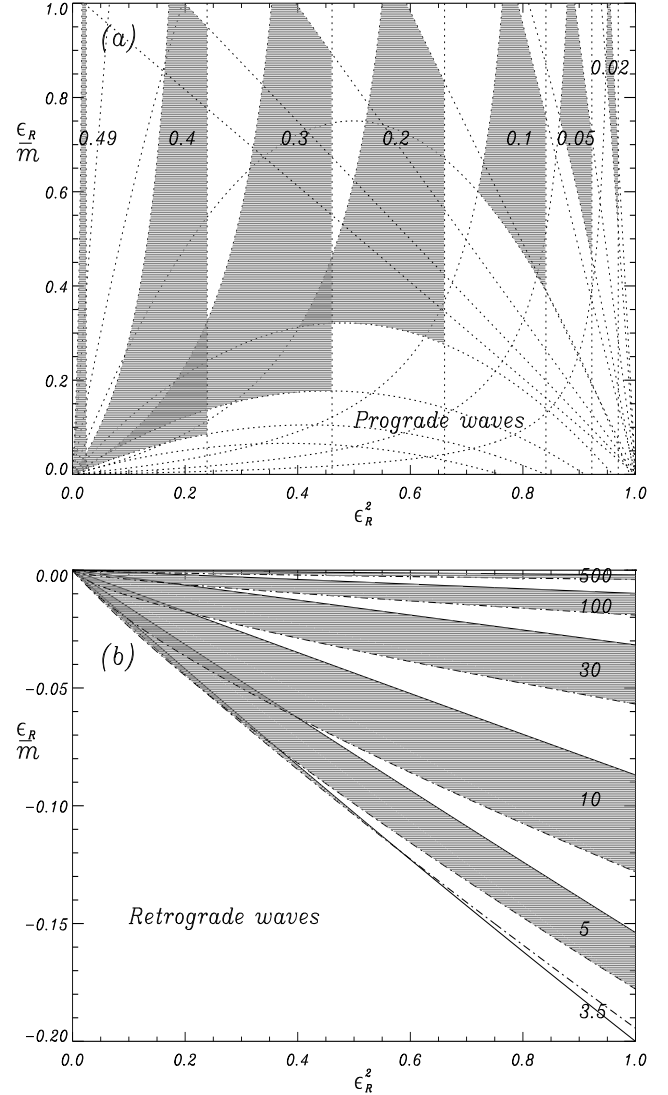


Fig. 2. The wave instability areas (hatched) in the phase space from an overlap of Figs. 1a and 1b. The labels in the areas are the β_μ values. Both prograde and retrograde waves β_μ are limited: for prograde waves the instability is possible if $\beta_\mu < 0.5$, for retrograde waves the instability is possible if $\beta_\mu > 3.5$.

is valid for $\epsilon_R^2 = 1$ and $\beta_\mu = 5/2$, which follows from Eq. (52).

The total condition for the existence of spatially stable but temporarily unstable waves reads as follows:

$$\chi_2 < \frac{\epsilon_R}{m} < \min(\chi_1, \chi_3). \quad (53)$$

Figs. 2a, b show the validity ranges of this condition for some typical values of β_μ . The hatched areas are places where LKHI is possible. These figures are obtained by overlapping the Figs. 1a and 1b. For prograde waves on both sides these hatched areas become very narrow: with decreasing β_μ the extent of the hatched area decreases and tends to the point $\{\epsilon_R, m\} = \{1, 1\}$. We will see that this is

the solar case. The hatched areas of LKHI disappear with decreasing β_μ . This means we have a lower limit $(\beta_\mu)_{\min}$.

For retrograde waves it is sufficient to write the condition as $\chi_2 < \varepsilon_R/m < \chi_3$. In Fig. 2a χ_2 is the dashed curve and χ_3 is the solid curve. LKHI is possible if $\beta_\mu > 3.5$ for $0 \geq \varepsilon_R/m \geq -0.2$.

In Fig. 2 the hatched areas means that only these hatched areas for given β_μ are possible, if LKHI takes place. Outside these hatched areas regular solutions are impossible. The case without LKHI (neutral oscillations) must be investigated separately.

4.4. Solar rotation profile

Let us consider at which places we might expect LKHI in the Sun. Unfortunately, it is not clear how the core rotates. Nevertheless some rotation gradients close to Sun's center might exist, and we could expect LKHI there. It is known from helioseismology that the radiative interior has a very small β_μ , but the exact value is unknown. We have better information on the rotation profile of the solar envelope, including the tachocline. Helioseismology data may be described by different approximate formulae. One of these is (Charbonneau et al. 1998)

$$\Omega(r, \theta) = \Omega_c + \frac{1}{2} [1 + \text{erf}(\Delta)] (\Omega_s(\theta) - \Omega_c), \quad (54)$$

$$\Omega_s = \Omega_{\text{eq}} + c_1 \cos^2 \theta + c_2 \cos^4 \theta, \quad \Delta = \frac{r - r_c}{w},$$

$$\Omega_c/2\pi = 432.8 \text{ nHz}, \quad \Omega_{\text{eq}}/2\pi = 460.7 \text{ nHz},$$

$$c_1 = -62.69 \text{ nHz}, \quad c_2 = -67.13 \text{ nHz},$$

where $r_c = 0.713R_\odot$ is the radius at the bottom of the convective zone, and $w = 0.025R_\odot$ is the tachocline thickness. We can easily check that our approximation $\tilde{\Omega}/\Omega_c \ll 1$ is always applicable, if Eq. (54) is represented by $\Omega = \Omega_c + \tilde{\Omega}(r, \theta)$. The maximum value $(\tilde{\Omega}/\Omega_c)_{\max} \approx 0.06$ for $\theta = \pi/2$ (equator) is in the convection zone. From Eq. (54) we find the latitudinal gradient of rotation

$$\beta_\mu = -\frac{1 + \text{erf}(\Delta)}{2\Omega} \sin^2 \theta (c_1 + 2c_2 \cos^2 \theta). \quad (55)$$

Our supposition about $\beta_\mu \approx \text{const}$ and $\beta_r \approx \text{const}$ is based on the presentation $\tilde{\Omega} \approx \Omega_1(r) + \Omega_2(\theta)$. We could receive such an approximate formula instead of Eq. (54), but we need only local values of the gradients for which Eq. (55) is acceptable. Using this formula we show in Fig. 3 the $\beta_\mu(\theta)$ dependence for different r/R_\odot . We see that in the Sun $\beta_\mu \leq 0.02$, and the maximum is in the photosphere. From Fig. 2 follows that the LKHI of retrograde waves is not present in the solar case. LKHI of prograde waves in the Sun occurs in the upper right corner of Fig. 2a which is enlarged in Fig. 4. Here we see that the LKHI area disappears when $\beta_\mu < 3 \cdot 10^{-4}$. This boundary is located at the bold horizon in Fig. 3. Thus the prograde waves become unstable in the Sun at those places where $3 \cdot 10^{-4} \leq \beta_\mu \leq 2 \cdot 10^{-2}$. It means that LKHI is possible in the area $r/R_\odot > 0.6725$ which includes the greatest

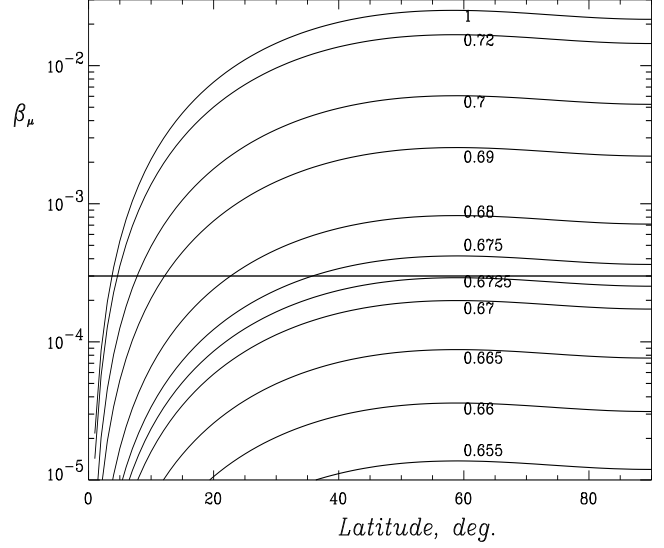


Fig. 3. The local estimate of the logarithmic gradient of the solar rotation frequency β_μ for real solar data from helioseismology depending on the co-latitude and the radial distance (the labels are values of r/R_\odot). The bold horizon is $\beta_\mu = 3 \cdot 10^{-4}$, above which the prograde waves become unstable (see next picture).

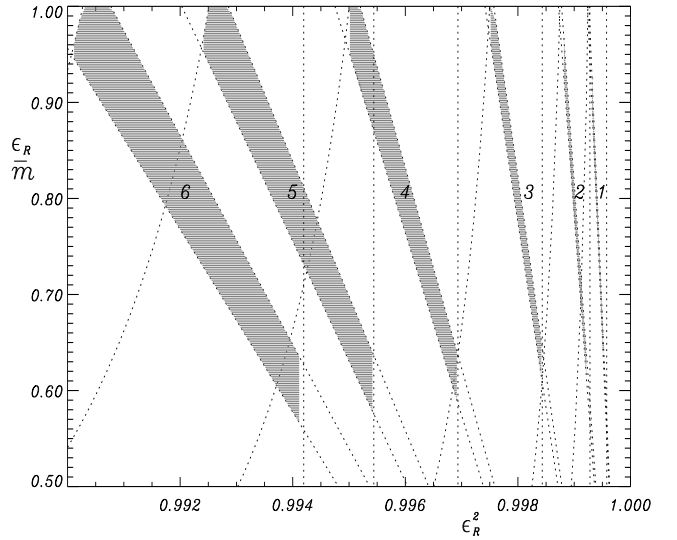


Fig. 4. Enlarged part of Fig. 2a for the smallest gradients of rotation. The labels 1, 2, ..., 6 correspond to $\beta_\mu = 3 \cdot 10^{-4}, 5 \cdot 10^{-4}, 1 \cdot 10^{-3}, 2 \cdot 10^{-3}, 3 \cdot 10^{-3}, 4 \cdot 10^{-3}$. Areas of instability exist only if $\beta_\mu \geq 3 \cdot 10^{-4}$.

part of the tachocline, the convective zone, and the photosphere. With increasing r the LKHI zone expands from middle to high latitudes. Figs. 2a and 4 show that LKHI is occurs at high frequencies ($\varepsilon_R \lesssim 1$) and in global scales ($\varepsilon_R/m > 0.5$). Considering that $m \neq 0$ is an integer we get $m = 1$.

However, our quantitative analysis of LKHI is based on the general Riemann scheme of Hein's equation, which

is valid only if the middle singular point $x = a$ is far from the other edges at $x = 0$ and $x = 1$. Thus, the limiting cases $\varepsilon_R \rightarrow 0$ and $\varepsilon_R \rightarrow 1$ (the latter is more important for solar LKHI) should be considered separately. In these limiting cases the regularity condition Eq. (48) may be changed, and the curve in Fig. 4 limiting the instability areas from below may be shifted. In this case LKHI with higher m -modes should be expected.

5. The low-frequency waves

After the qualitative analysis of Heun's Eq. (45) we can start a quantitative analysis. Note that the qualitative conclusions drawn above are valid for the more general Eq. (34) with Λ term. Heun's equation with four singularities in the general case is solved by a series of hypergeometric Gauss functions. A similar task has been considered for the damping of MHD waves at resonance levels by Dzhililov & Zhugzhda (1990). We will start to study Eq. (45) for some simple limiting cases. At high frequencies ($\varepsilon_R^2 \approx 1$, when LKHI is acting in the Sun) and at low frequencies ($\varepsilon_R^2 \ll 1$, when the waves are stable against LKHI in the Sun) Heun's equation is strongly simplified. In these cases the singular level $x = a$ is shifted either to the pole or to the equator. For both cases solutions are expressed by one hypergeometric function.

In the present work we consider particularly the second case. Let $\varepsilon_R^2 \ll 1 + \beta_\mu$. Then we have $a \approx 1$ and $h \approx 1$. Eq. (45) is now the hypergeometric equation:

$$x(1-x)Y'' + [\gamma - (\tilde{\alpha} + \tilde{\beta} + 1)x]Y' - \tilde{\alpha}\tilde{\beta}Y = 0, \quad (56)$$

where all parameters are defined by Eqs. (42, 44, 47). In these definitions ε_R^2 should set to zero. Then the Θ -part of the pressure perturbations, Eq. (41), is expressed by two Gaussian hypergeometric functions:

$$\Theta = C_1 x^{\sigma_1} Y_1(x) + C_2 x^{\sigma_2} Y_2(x). \quad (57)$$

$$\text{Here } Y_{1,2}(x) = F(\tilde{\alpha}, \tilde{\beta}; \gamma; x)|_{\sigma=\sigma_{1,2}}, \quad (58)$$

and $C_{1,2}$ are arbitrary constants. This general solution includes LKHI for larger β_μ too. This could be realized perhaps in other, younger stars. For the Sun we have $\beta_\mu \ll 1$. We will finish this paper by considering in detail the more popular case when rotation is uniform, $\beta_\mu = 0$.

5.1. Rigid rotation case

Using the conditions $\beta_\mu = 0$ and $\varepsilon_R^2 \ll 1$ the parameters in the solution Eq. (57) are strongly simplified. Because $2\sigma = \pm|m|$ only a regular solution at the pole ($x = 0$) will be left. In the standard definitions of hypergeometric functions (Abramowitz & Stegun 1984) we have

$$\Theta = Cx^{|m|/2}F(a, b; c; x), \quad (59)$$

$$a = \frac{1}{2} \left(-\frac{1}{2} + |m| + q \right), \quad b = \frac{1}{2} \left(-\frac{1}{2} + |m| - q \right),$$

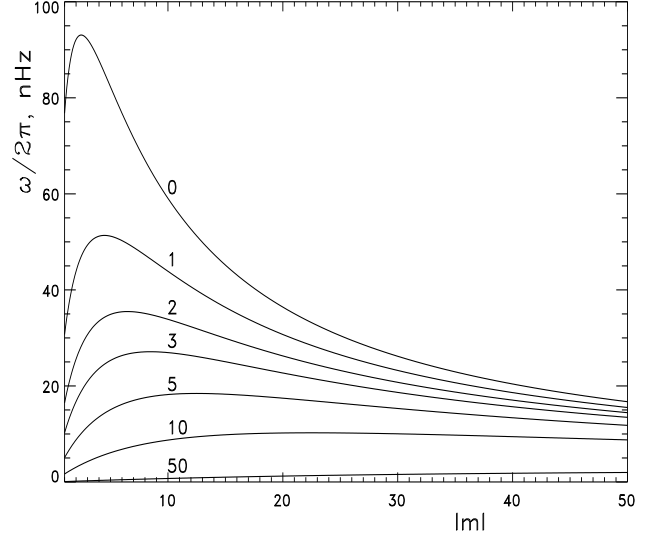


Fig. 5. The spectrum $\omega(l, m)$ of low-frequency retrograde modes. The numbers at the curves are the l values. For the calculation of the spectrum, Eq. (66), $\Omega = \Omega_{\text{eq}} = 460.7$ nHz is used.

$$c = 1 + |m|, \quad q = \sqrt{\frac{1}{4} - \frac{m}{\varepsilon_R}}, \quad \text{and } C = \text{const.}$$

Note that $c - a - b = 3/2$. The analytical continuation of the solution Eq. (59) to the equator, $x \rightarrow 1$, gives

$$\Theta = Cx^{|m|/2} \left[AF(a, b; -\frac{1}{2}; 1-x) + B(1-x)^{3/2} F(c-a, c-b; \frac{5}{2}; 1-x) \right]. \quad (60)$$

Here the continuation coefficients are (Abramowitz & Stegun 1984)

$$A = \frac{\Gamma(c)\Gamma(3/2)}{\Gamma(c-a)\Gamma(c-b)} = F(a, b; c; 1), \quad (61)$$

$$B = \frac{\Gamma(c)\Gamma(-3/2)}{\Gamma(a)\Gamma(b)}. \quad (62)$$

Eqs. (59, 60) mean that pressure is limited everywhere in the hemisphere. Now let us consider the velocity components. Putting Eq. (59) into Eq. (39) we get

$$V_\theta = \pm \frac{CQ\varepsilon_R^2}{r\rho_0 i\omega} \frac{x^{|m|/2}}{\sqrt{x(1-x)}} \left[\left(\frac{m}{\varepsilon_R} - |m| \right) F(a, b; c; x) - x \frac{2ab}{c} F(a+1, b+1; c+1; x) \right]. \quad (63)$$

Taking into account that $F(a, b; c; 0) = 1$, we receive from the regularity of V_θ at $x = 0$ that $|m| \geq 1$. Axially-symmetric waves $m = 0$ cannot be formed. The continuation of the solution Eq. (63) to the equator, $x \rightarrow 1$, gives

$$V_\theta = \pm \frac{CQ\varepsilon_R^2}{r\rho_0 i\omega} x^{(|m|-1)/2} \left(\frac{A}{\sqrt{1-x}} \mathcal{L}_1 + B\mathcal{L}_2 \right), \quad (64)$$

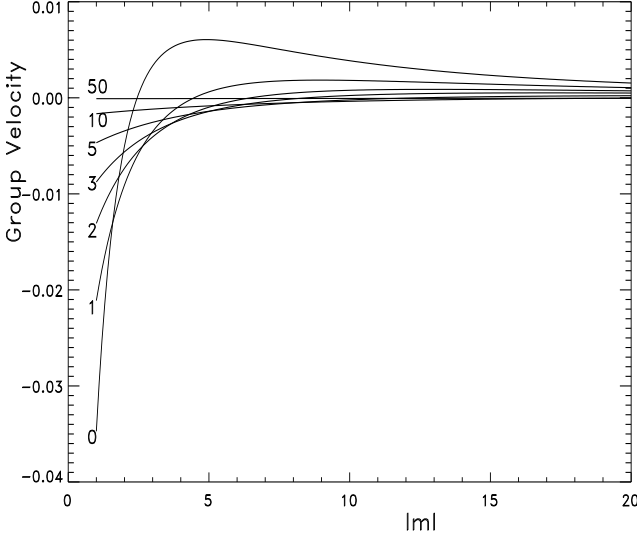


Fig. 6. The normalized group velocity $v_g/2\Omega r_0 \sin \theta_0$ as a function of the azimuthal numbers for given degrees l .

$$\begin{aligned} \mathcal{L}_1 &= \left(\frac{m}{\varepsilon_R} - |m| \right) F\left(a, b; -\frac{1}{2}; 1-x\right) - \\ &\quad - x4abF\left(a+1, b+1; \frac{1}{2}; 1-x\right), \\ \mathcal{L}_2 &= \left[\left(\frac{m}{\varepsilon_R} - |m| \right) (1-x) + 3x \right] F\left(c-a, c-b; \frac{5}{2}; 1-x\right) + \\ &\quad + \frac{4}{5}x(1-x)(c-a)(c-b)F\left(c-a+1, c-b+1; \frac{7}{2}; 1-x\right). \end{aligned}$$

As for $x = 1$ the functions \mathcal{L}_1 and \mathcal{L}_2 are limited, we have the relation $A \equiv 0$ from the regularity requirement. Using a property of the gamma-functions (its presentation as an infinite product) in Eq. (61) we get the condition of quantization

$$q^2 = \left(2l + |m| + \frac{5}{2} \right)^2, \quad l = 0, 1, 2, \dots \quad (65)$$

From here we get the simple dispersion relation

$$\frac{\varepsilon_R}{m} = \frac{1}{m} \frac{\omega}{2\Omega} = -\frac{1}{(2+2l+|m|)(3+2l+|m|)}. \quad (66)$$

Since $\varepsilon_R/m < 0$ for any $l \geq 0$, only retrograde modes (as seen in the rotating frame) are possible.

5.1.1. Spectrum of retrograde modes

The new dispersion relation Eq. (66) completely differs from the dispersion relation of the almost toroidal r-modes. Their dispersion relation can be derived from Eq. (66) if we formally set $l_s = 2(1+l) + |m|$. Then

$$\omega = -2\Omega \frac{m}{l_s(1+l_s)}. \quad (67)$$

However, here the degrees l_s are functions of m . Due to the coupling of the modes in our case the eigenfunctions can

never be expressed by the associated Legendre functions $P_{l_s}^m$. For the r -modes the axi-symmetric modes ($m = 0$) with $\omega = 0$ are possible, while our case rejects this case. Unlike the r -modes the spectrum Eq. (66) has a maximum at $m^2 = m_0^2 = 2(1+l)(3+2l)$. If $l \gg 1$ we have $|\varepsilon_R|_{\max} \approx 1/8l$. The spectrum of retrograde waves is shown in Fig. 5. Rossby waves in geophysics (Pedlosky 1982) have a similar spectrum. Using Eq. (66) we may define the local phase and group velocities (at fixed latitude θ_0 and radial distance r_0) in the azimuthal plane

$$v_{\text{ph}} = -\frac{2\Omega r_0 \sin \theta_0}{(2+2l+|m|)(3+2l+|m|)}, \quad (68)$$

$$v_{\text{gr}} = 2\Omega r_0 \sin \theta_0 \frac{m^2 - 2(1+l)(3+2l)}{(2+2l+|m|)^2(3+2l+|m|)^2}. \quad (69)$$

We see that the group velocity changes its sign at the maximum of the spectrum, where $m^2 = m_0^2$. Fig. 6 shows that the $l = 0$ mode has a maximum group velocity. Long waves carry energy opposite to the rotation direction, while a packet of short waves is carried in rotation direction. The facts that the frequencies $\omega(m)$ have a maximum (two different $|m|$ correspond to the same ω) and at the maximum of $\omega = \omega_{\max}$ the group velocity changes the direction hints at the existence of two branches of oscillations. Solving Eq. (66) for $|m|$ we get these branches. Let $\omega > 0$ and $m = -|m|$. Then

$$|m| = \frac{1}{2\varepsilon_R} (w_1 \mp \sqrt{w_2}) = m_{1,2}, \quad (70)$$

$$w_1 = 1 - \varepsilon_R - 4\varepsilon_R(1+l),$$

$$w_2 = (1 - \varepsilon_R)^2 - 8\varepsilon_R(1+l).$$

From here we get an upper limit for l if ε_R is given: $l \leq l_{\max} = (1 - \varepsilon_R)^2 / 8\varepsilon_R - 1$. For such degrees of l the azimuthal numbers are also limited: $m_1 \leq |m| \leq m_2$. For $\varepsilon_R \rightarrow 0$ we have $l_{\max} \rightarrow 1/8\varepsilon_R$, $m_2 \rightarrow 1/\varepsilon_R$, and $m_1 \rightarrow 0$. However, considering the regularity of the solutions Eq. (63), we must take $m_1 \geq 1$. From here we get the lower limit of l :

$$l \geq l_{\min} = \frac{1}{4} \left(\sqrt{1 + \frac{4}{\varepsilon_R}} - 7 \right). \quad (71)$$

Since $l \geq 0$, we get $\varepsilon_R \leq 1/12$ from Eq. (71). For $\varepsilon_R = 1/12$ we have $l_{\min} = 0$. Thus the eigenmodes exist for $\varepsilon_R \leq 1/12$ if $l_{\min} \leq l \leq l_{\max}$ and $m_1 \leq |m| \leq m_2$. For $l = l_{\max}$ we have $m_1 = m_2$, and $m_1 = 1$ for $l = l_{\min}$. This situation is shown in Fig. 7 for different values of ε_R . A decrease of the frequency decreases the domain of the existence of the modes.

Setting Eq. (70) into Eqs. (68, 69) gives

$$\frac{v_{\text{ph}}^{\pm}}{2\Omega r_0 \sin \theta_0} = -\frac{w_1 \pm \sqrt{w_2}}{4(1+l)(3+2l)}, \quad (72)$$

$$\frac{v_{\text{gr}}^{\pm}}{2\Omega r_0 \sin \theta_0} = -\frac{w_2 \pm w_1 \sqrt{w_2}}{4(1+l)(3+2l)}. \quad (73)$$

Here v_{ph}^+ is the phase velocity of the fast modes and v_{ph}^- that of the slow modes. For $l = l_{\max}$ we have $v_{\text{gr}}^{\pm} = 0$

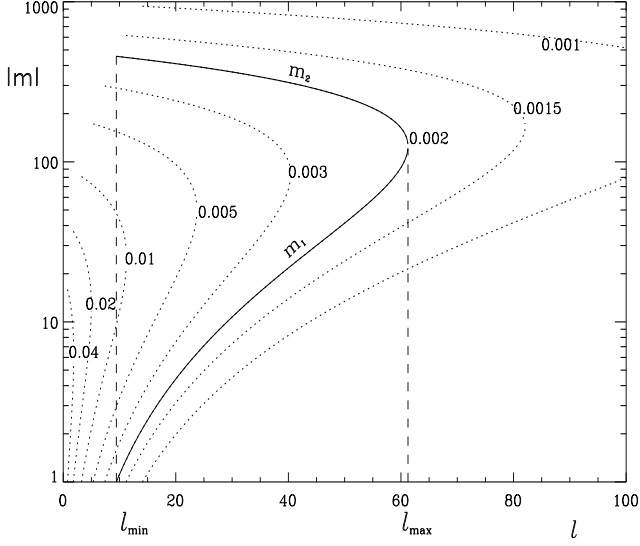


Fig. 7. The possible domain of the existence of eigenmodes for given Rossby numbers ε_R (the numbers at the curves). For example, the case $\varepsilon_R = 0.002$ (close to the 22-year modes) is emphasized. All possible values of the azimuthal numbers ($m = m_1$ and $m = m_2$) are on this curve for given discrete l in the range $l_{\min} \leq l \leq l_{\max}$ (see text). If $\varepsilon_R > 1/12$, the eigenmodes disappear.

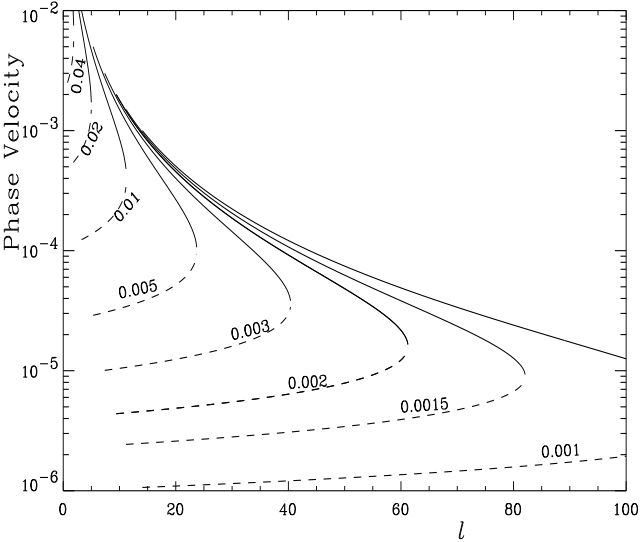


Fig. 8. The phase velocities of fast (solid) and slow (dashed curves) modes versus l . The numbers at the curves are ε_R values, similar to Fig. 7. Here the velocities are normalized to $(-2\Omega r_0 \sin \theta_0)$. Every curve is restricted to the range $l_{\min} \leq l \leq l_{\max}$.

and $v_{\text{ph}}^+ = v_{\text{ph}}^-$. In Eq. (70) and in Fig. 7 the m_1 branch corresponds to the fast mode, but m_2 to the slow modes, since $m_2 \geq m_1$. In Fig. 8 the normalized phase velocities (with inverse sign) for the selected values of ε_R in Fig. 7 are shown versus l . Both branches are retrograde modes ($v_{\text{ph}}^{\pm} < 0$). Using $\Omega R_{\odot} \sim 2$ km/s for the Sun, we get from Fig. 8 very slow phase velocities. The fast wave velocity

(solid lines) depends more strongly on l . With increasing ε_R both branches are accelerated.

In Fig. 9 the group velocities are presented in the same way. For fast waves the group velocity is always parallel to the phase velocity ($v_{\text{gr}}^+ < 0$), while for the slow waves we have the opposite behavior $v_{\text{gr}}^- > 0$. Slow modes packets carry off energy in the rotation direction. Always $|v_{\text{gr}}^+| > |v_{\text{gr}}^-|$ is valid. With decreasing ε_R the range $[l_{\min}, l_{\max}]$ is shifted to the right-hand side, and it is seen in Fig. 9 that v_{gr}^- for such low ε_R is almost zero.

Note that $m = l$ modes are always fast modes.

5.1.2. The eigenfunctions

Taking into account the quantization condition Eq. (65) in the solutions Eqs. (60, 64, 38, and 40) we obtain the eigenfunctions. Turning from complex velocities into the real displacements, $\mathbf{V} = -i\omega\xi$ (recall that \mathbf{V} is the velocity seen in the rotating frame), we get

$$p' = Q(r)\Theta(\theta) \cos \left[m \left(\phi - 2\frac{\varepsilon_R}{m}\Omega t \right) \right], \quad (74)$$

$$\xi_{\theta} = \xi_{\theta}^* \cos \left[m \left(\phi - 2\frac{\varepsilon_R}{m}\Omega t \right) \right], \quad (75)$$

$$\xi_{\phi} = \xi_{\phi}^* \sin \left[m \left(\phi - 2\frac{\varepsilon_R}{m}\Omega t \right) \right], \quad (76)$$

$$\xi_r = \xi_r^* \cos \left[m \left(\phi - 2\frac{\varepsilon_R}{m}\Omega t \right) \right]. \quad (77)$$

Here the amplitude functions are

$$\xi_r^* = \frac{1}{\omega^2 - N^2} \frac{\Theta}{\rho_0} \frac{dQ(r)}{dr}, \quad (78)$$

$$\xi_{\theta}^* = \frac{Q(r)}{4\Omega^2 r \rho_0} \xi_{\theta A}(\theta), \quad (79)$$

$$\xi_{\phi}^* = \frac{Q(r)}{4\Omega^2 r \rho_0} \xi_{\phi A}(\theta). \quad (80)$$

The amplitudes are expressed by Jacobi's polynomials:

$$\Theta = B(\sin \theta)^{|m|} \cos^3 \theta F_1(\theta), \quad (81)$$

$$\xi_{\theta A} = B(\sin \theta)^{|m|-1} \cos^2 \theta \left(\frac{m}{\varepsilon_R} F_1 - \frac{4lk}{5} \sin^2 \theta F_2 \right), \quad (82)$$

$$\xi_{\phi A} = -\frac{B}{\varepsilon_R} \frac{2lk}{5} \sin(2\theta) \cos^2 \theta (\sin \theta)^{|m|} F_2(\theta), \quad (83)$$

$$F_1 = F \left(-l, k; \frac{5}{2}; \cos^2 \theta \right) = \quad (84)$$

$$= (-1)^l \frac{l! \Gamma(5/2)}{\Gamma(l+5/2)} P_l^{(|m|, 3/2)}(\cos 2\theta) =$$

$$= \sum_{j=0}^l \frac{(-l)_j (k)_j}{(5/2)_j j!} (\cos \theta)^{2j},$$

$$F_2 = F \left(1-l, 1+k; \frac{7}{2}; \cos^2 \theta \right) = \quad (85)$$

$$= (-1)^{l-1} \frac{(l-1)! \Gamma(7/2)}{\Gamma(l+5/2)} P_{l-1}^{(1+|m|, 5/2)}(\cos 2\theta) =$$

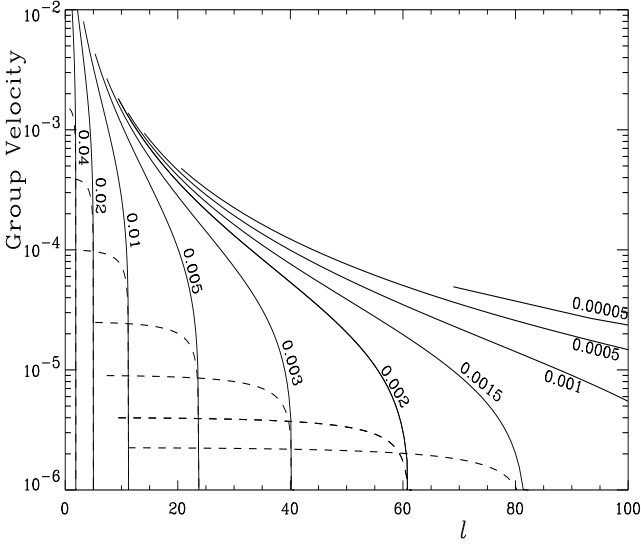


Fig. 9. Absolute values of the group velocities of fast (solid) and slow (dashed curves) modes normalized to $2\Omega r_0 \sin \theta_0$ versus l for selected ε_R . For fast waves $v_{\text{gr}}^+ < 0$, for slow modes $v_{\text{gr}}^- > 0$. For $l = l_{\text{max}}$ we have $v_{\text{gr}}^+ = v_{\text{gr}}^- = 0$.

$$= \sum_{j=0}^{l-1} \frac{(1-l)_j (1+k)_j}{(7/2)_j j!} (\cos \theta)^{2j}.$$

$$k = \frac{5}{2} + |m| + l, \quad (f)_j = \frac{\Gamma(f+j)}{\Gamma(f)}, \quad (86)$$

and $F_2 \equiv 0$ if $l = 0$. The eigenfunctions of the retrograde low-frequency modes Eqs. (74–77) are written for the hemisphere $0 \leq \theta \leq \frac{\pi}{2}$. In the other hemisphere we have to change $\cos \theta$ to $|\cos \theta|$ and to change the sign of ξ_θ . We put $C = 1$ because all eigenfunctions are multiplied by the solution of the r -Eq. (32). Changing the sign of m the function ξ_ϕ keeps its sign because $\varepsilon_R/m < 0$. It follows from Eqs. (84, 85) that the eigenfunctions are represented by a limited number of trigonometric functions. The number of terms is defined by l in the range $l_{\text{min}} \leq l \leq l_{\text{max}}$. This is qualitatively different from the presentation of the rotation-mode eigenfunctions by infinite series of spherical harmonics.

Let us consider some particular cases.

- Pole ($\theta = 0$): taking into account $BF_1 = 1$ we have $\Theta = p' = \xi_r = \xi_\phi = 0$. $\xi_\theta = 0$ if $|m| > 1$. For $|m| = 1$ we have $\xi_{\theta A} = -2(3+2l)(2+l)$.
- Equator ($\theta = \frac{\pi}{2}$): here $F_1 = F_2 = 1$ and $p' = \xi_\theta = \xi_\phi = 0$.
- $l = 0$ case: then $B = F_1 = 1$, $F_2 = 0$,

$$\Theta = (\sin \theta)^{|m|} \cos^3 \theta,$$

$$\xi_{\theta A} = -(2+|m|)(3+|m|) \cos^2 \theta (\sin \theta)^{|m|-1},$$

and $\xi_\phi = 0$ (in our $\varepsilon_R^2 \ll 1$ limit).

- $l \gg |m|$, $|m|$ is not large, and $\theta \neq 0, \frac{\pi}{2}$ as well.

The latter case is important because the range $l_{\text{min}} \leq l \leq l_{\text{max}}$ is large for small ε_R^2 . Remember that for $\varepsilon_R = 1/12$ we have $l_{\text{min}} = 0$. Using the asymptotic formula for Jacobi's polynomial (or the hypergeometric function) of large degree we have

$$\Theta \simeq \frac{|m|! \cos \lambda \cos \theta}{\sqrt{\pi l} l^{|m|} \sqrt{\sin \theta}}, \quad (87)$$

$$\xi_{\theta A} \simeq \frac{|m|! \cos \lambda}{\sqrt{\pi l} l^{|m|} (\sin \theta)^{3/2}} \left(\frac{m}{\varepsilon_R} + \frac{14}{5} k \tan \theta \tan \lambda \right), \quad (88)$$

$$\xi_{\phi A} \simeq \frac{14}{5} \frac{|m|! k \sin \lambda}{\varepsilon_R \sqrt{\pi l} l^{|m|} \sqrt{\sin \theta}}. \quad (89)$$

$$\lambda = \left(2l + \frac{5}{2} + |m| \right) \theta - \frac{\pi}{2} \left(|m| + \frac{1}{2} \right).$$

These extremely simple asymptotic formulae for the eigenfunctions might be used in most cases. The formula for the case of large l with large $|m|$ also could be found, e.g. in the book of Bateman & Erdélyi (1953).

In Fig. 10 for some typical selected (l, m) pairs the amplitude functions, Eqs. (81–83), are shown as function of θ . The first row is the pressure $\Theta(\theta)$ function normalized to its maximum. The first $l = 1$ window represents Θ for different $|m|$ (increasing $|m|$ from left to right). As the eigenfunctions are multiplied by a $\sin^{|m|} \theta$ factor, the amplitudes are strongly suppressed around the pole. Increasing $|m|$ for a given l shifts the maximums toward the equator. l is the surface node number of the $\Theta(\theta)$ function. Increasing l for given $|m|$ (the second window of pressure with $m = 1$ in Fig. 10) contrarily suppresses the amplitudes around the equator, and the maximum is shifted toward the pole. $l = |m|$ is the equilibrium case. In the third window of pressure the balance latitude with a maximum amplitude is defined by $\theta = 20^\circ$ for all $l = |m|$ modes.

The second and third rows of Fig. 10 are the latitudinal ($\xi_{\theta A}$) and azimuthal ($\xi_{\phi A}$) eigenfunction amplitudes, respectively, normalized to the maximum of $\xi_{\theta A}$, see Eqs. (79, 80). The latitudinal amplitude behavior is similar that of the pressure. The azimuthal amplitudes are smaller than the latitudinal amplitudes, but with a change of l a redistribution of the amplitudes will not take place. $\xi_{\phi A}$ has practically the same amplitude at all latitudes and for all l .

From Fig. 10 follows that we can expect an interesting behavior of the eigenfunction amplitudes, when both l and $|m|$ are large. A suppression from two sides may evoke a concentration of wave energy in narrow latitudinal bands. For example, this is the case for the 22-year solar mode.

For the 22-year modes we take $\omega_{22} = 2\pi(1.441 \text{ nHz})$, for which $\varepsilon_R \approx 0.0016$. Then we derive from Eq. (71) the limiting values of the integer l , $11 \leq l \leq 76$. For all l in this range we find from Eq. (70), rounding off, integer azimuthal numbers m_1 and m_2 for the fast and slow modes, respectively. Putting these integer numbers into Eq. (66) we find the deviation $\delta = \omega_{22} - \omega$ from the central frequency due to the integer azimuthal numbers. The results are given in Table 1 in Appendix A. It is seen that the

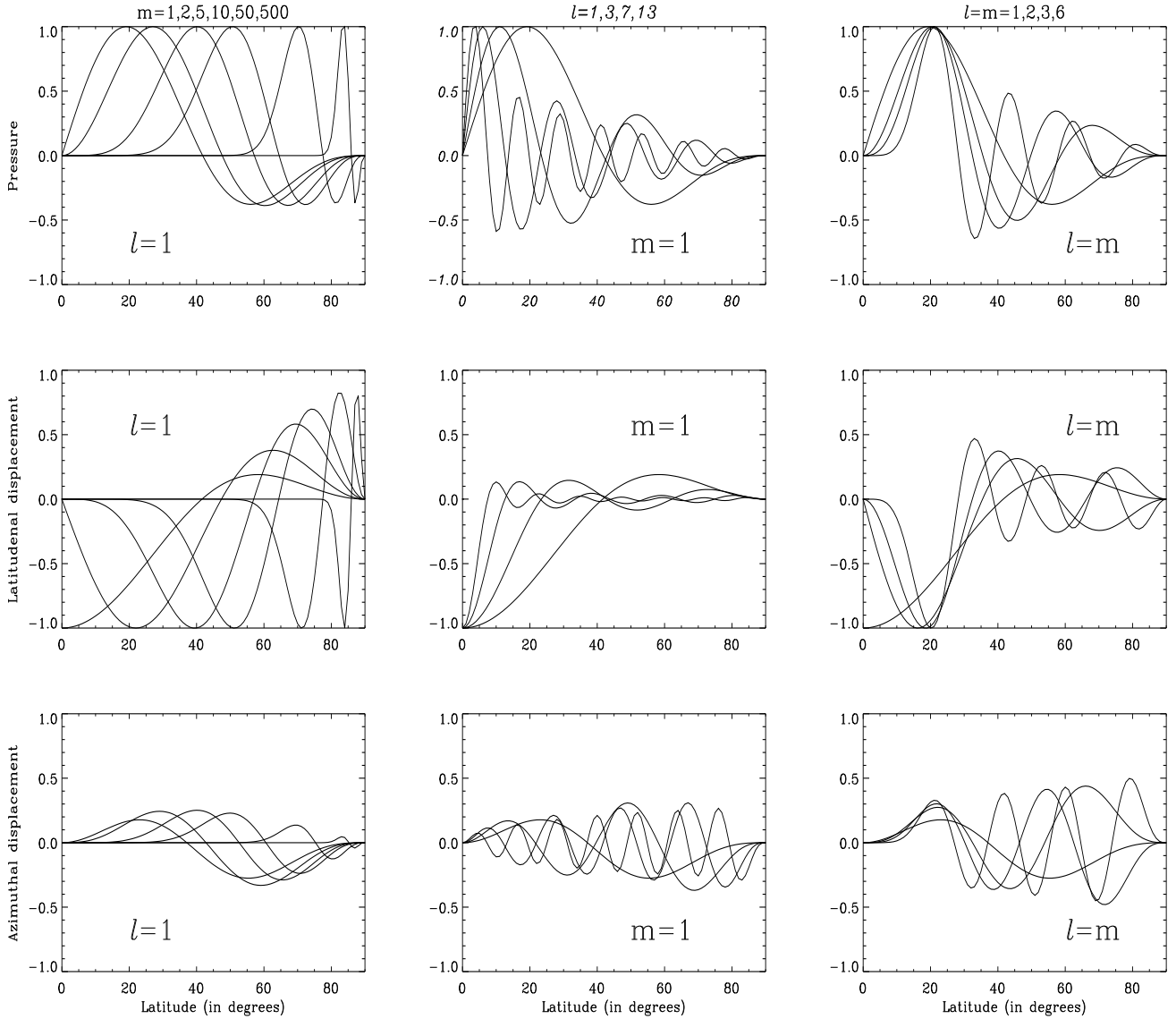


Fig. 10. The amplitudes of eigenfunctions versus latitude for given pairs $(l, |m|)$, Eqs. (81)–(83). The pressure row shows the $\Theta(\theta)$ function normalized to its own maximum. From left to right all curves are related to the wave numbers given above. The middle and last rows are similar to the first row, but show now the latitudinal ($\xi_{\theta A}$) and azimuthal ($\xi_{\phi A}$) amplitude functions, normalized to the maximum of ($\xi_{\theta A}$).

fast modes with low l have larger deviations. This table includes all possible $(l, |m|)$ pairs which correspond to the 22-year period. For some example pairs of $(l, |m|)$ we plot in Fig. 11 the latitude dependence of the quantity $(\xi_{\theta}^2 + \xi_{\phi}^2)^{1/2}$, averaged over the wave period, which characterizes the energy density of the modes. The hemisphere is divided into two equal parts: slow modes are located around the equator (solid lines), fast modes are concentrated around the pole. Each $(l, |m|)$ pair is located in a narrow latitudinal band. Note that the slow modes (the group velocity of which is in the rotation direction) with sunspot-like spatial scales are at latitudes of $30 - 40^\circ$ from the equator.

5.1.3. Flow patterns

The eigenfunctions Eqs. (74)–(77) allow us to discuss the flow character produced by the waves, even if the solution of the radial equation $Q(r)$ is unknown. Excluding from these equations the time-dependent phase we can receive the trajectory equations of the fluid elements. In the meridional $(\mathbf{r}, \boldsymbol{\theta})$ plane we have

$$\frac{\xi_{\theta}}{\xi_r} = \varepsilon_R^2 \frac{Q(r)\psi(r)}{rQ'(r)} \frac{\xi_{\theta A}}{\Theta} = \tan(\alpha_r). \quad (90)$$

It follows from here that the motion in the meridional plane is linear. The poloidal displacement vector in the meridional plane is inclined to the radius by an angle α_r . For $\alpha_r \approx \frac{\pi}{2}$ we have meridional flows and for $\alpha_r \approx 0$ radial flows. However, since $\xi_{\theta}/\xi_r \sim 1/\sin(2\theta)$, for any r

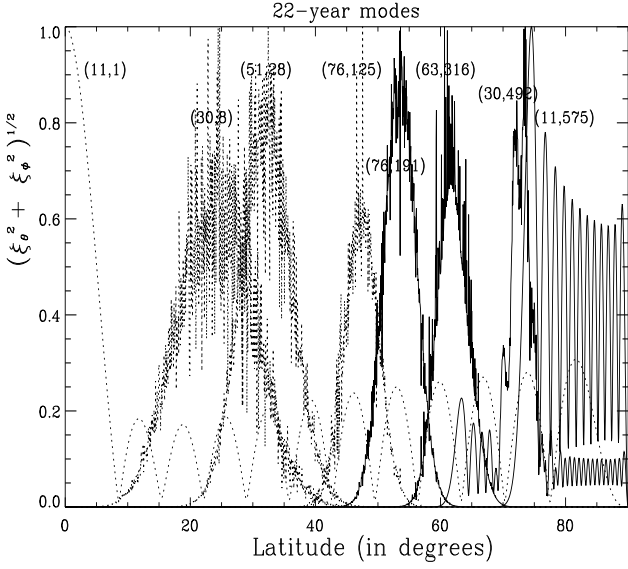


Fig. 11. The normalized energy density of the 22-year fast (dashed) and slow (solid) modes versus co-latitude. The numbers at the curves are $(l, |m|)$ pairs taken from Table 1.

the motions around the pole and around the equator will be almost meridional ($|\xi_\theta| \gg |\xi_r|$). We see from Eq. (90) also that the direction of the flow vector will be changed to $\pi/2$ if we pass along the radius from the node of the $Q(r)$ -function to $Q'(r)$. Note that every node of $Q'(r)$ is located between the neighbouring two nodes of $Q(r)$. For large radial numbers (such orders are expected) these nodes are located close to each other. Then we have a complicated motion in the meridional plane.

At the surface of the cone over (\mathbf{r}, ϕ) the trajectory of each fluid element is an ellipse around the equilibrium point. The cone displacement equation is

$$\frac{\xi_\phi^2}{\xi_\phi^{*2}} + \frac{\xi_r^2}{\xi_r^{*2}} = 1. \quad (91)$$

The ratio of the semiaxes ξ_ϕ^* and ξ_r^*

$$\frac{\xi_\phi^*}{\xi_r^*} = -\varepsilon_R \frac{Q(r)\psi(r)}{rQ'(r)} \frac{4lk}{5} \frac{F_2}{F_1} \sin \theta \quad (92)$$

means that close to the axis of rotation the flow is directed along this axis. On the bigger cone through the equator, where $F_1 = F_2 = 1$, the motion is mainly azimuthal since $lk > 1$. An exception are in this case the nodes of the $Q(r)$ -function at the radius. For large $l \gg 1$ the ratio $\xi_\phi^*/\xi_r^* \sim \tan(2l\theta)/\cos\theta$ means that the character of the flows is changing at middle latitudes.

At the surface of any sphere with a radius r the motion of the fluid elements is on trajectories of the ellipse

$$\frac{\xi_\theta^2}{\xi_\theta^{*2}} + \frac{\xi_\phi^2}{\xi_\phi^{*2}} = 1. \quad (93)$$

Here the ratio of the semiaxes is independent of the radius:

$$\frac{\xi_\phi^*}{\xi_\theta^*} = -\frac{4lk}{5\varepsilon_R} \sin^2 \theta \cos \theta \frac{F_2}{\frac{m}{\varepsilon_R} F_1 - \frac{4lk}{5} F_2 \sin^2 \theta}. \quad (94)$$

It is seen that near the equator and near the pole the motion is mainly in \mathbf{e}_θ direction. For large $l \gg 1$ this ratio is

$$\frac{\xi_\phi^*}{\xi_\theta^*} \simeq \frac{14k}{5\varepsilon_R} \frac{\sin \theta \tan \lambda}{\frac{m}{\varepsilon_R} + \frac{14}{5} k \tan \theta \tan \lambda}. \quad (95)$$

The flow pattern considered here drifts opposite to the sense of rotation with a speed v_{ph} , if it is observed in a frame rotating with the star.

6. Conclusions

In the present work we have derived the general PDE governing non-radial, adiabatic, long-period (with respect to the rotation period), linear oscillations of a slowly and differentially rotating star. This general equation includes all the high-order g -modes and all possible hybrids of rotation modes as well as their mutual interaction. The geophysical ‘traditional approximation’ considerably simplifies this general equation, and we get two ODEs for the r - and θ -components instead of one with arbitrary gradients of rotation $\Omega(r, \theta)$. We have received a more stringent condition for the applicability of this approximation to the pulsation of stars. Only for very low frequencies this restriction is the same as that of the standard case.

The θ -equation is Laplace’s equation generalized to the latitudinal differential rotation. Without solving this equation qualitatively we found the exact condition for the appearance of a global instability. This instability is driven by the latitudinal shear, it is not influenced by buoyancy. We call that a ‘latitudinal Kelvin-Helmholtz instability’ (LKHI). The appearance of LKHI strongly depends on the Rossby number (the ratio of rotation period and period of motion), on the azimuthal wave numbers and on the latitudinal rotation gradients. Very large gradients produce retrograde waves (seen in the rotating frame), while a slower rotation gradient is responsible for prograde mode LKHI. The rotation gradient has a lower boundary below which LKHI is not possible for any Rossby number or azimuthal number m .

We have applied the LKHI condition to the helioseismological data of the Sun. Here a global LKHI is possible for the $m = 1$ mode at practically all latitudes. Radially the LKHI is extended from the greatest part of the tachocline up to the photosphere. The LKHI for the Sun was first obtained by Watson (1981). According to his results the instability is possible only at photosphere layers. Later Gilman & Fox (1997) have shown that such an instability is possible in the tachocline too, if strong toroidal magnetic fields are included. Our results show that the instability of the $m = 1$ modes and other modes is possible without magnetic fields, in contradiction to Gilman & Fox (1997). This difference is probably connected with the incompleteness of the equations used by

Watson (1981) and by Gilman & Fox (1997); their equations are two-dimensional only.

The exact solutions of Laplace's tidal equation for lower frequencies are expressed by Jacobi's polynomials. Just for lower frequencies the numerical calculations of stellar pulsation analyses meet great problems, when looking for the eigenfunction as infinite series of Legendre functions. The eigenfunctions, defined by higher-order polynomials of Jacobi, cannot be expressed by convergent series of associated Legendre functions. Every Legendre function is a particular case of a Jacobi polynomial.

It has been shown here that the retrograde (slow and fast) modes with high surface wave numbers (l, m) are energetically concentrated in narrow bands of latitudes. This analysis was done for the 22-year modes as an example. Such a concentration of mode energy in a narrow spatial area makes such modes vulnerable to different instability mechanisms such as the ε -mechanism considered in Paper 1.

Appendix A: Coefficients of the main equation

In Section 2.2 our main Eq. (26) for the pressure perturbations has been derived:

$$[\psi_1 \check{\delta}_r^2 + \psi_2 \check{\delta}_\mu^2 + \psi_3 \check{\delta}_r + \psi_4 \check{\delta}_\mu + \psi_5 \check{\delta}_r \check{\delta}_\mu + \psi_6] \tilde{P} = 0. \quad (\text{A.1})$$

This singular PDE has the following coefficients:

$$\begin{aligned} \psi_1 &= 1 - \frac{N^2}{\omega^2} - j\mu^2 \frac{1 + \beta_r}{\alpha}, \\ \psi_2 &= \psi_1 \frac{1 - \mu^2}{\alpha} \left[\frac{\epsilon_R^2}{\mu^2} \left(1 - \frac{N^2}{\omega^2} \right) - j(1 + \beta_r) \right], \\ \psi_3 &= f_1 + \psi_1 f_2, \\ \psi_4 &= \frac{\psi_1^2}{\mu^2} \left[\frac{a_7}{a_3} + (1 - \mu^2) \left(\check{\delta}_\mu \frac{1}{a_3} - \frac{a_5}{a_3} \right) \right] + \\ &\quad + j [a_9 \psi_1 (f_2 - \check{\delta}_\mu a_3^*) - f_1 a_3^* - \psi_1 \check{\delta}_r a_3^*], \\ \psi_5 &= j\psi_1 \frac{1 - \mu^2}{\alpha} (2 + \beta_r + \beta_\mu), \\ \psi_6 &= f_1 f_2 + \psi_1 (\check{\delta}_r f_2) + j\psi_1 a_9 (\check{\delta}_\mu f_2) - \\ &\quad - \frac{\psi_1^2}{\mu^2} \left[m^2 + \frac{a_7 a_5}{a_3} + (1 - \mu^2) \check{\delta}_\mu \left(\frac{a_5}{a_3} \right) \right], \end{aligned}$$

where

$$\begin{aligned} f_1 &= \psi_1 (2 + ja_8) - \check{\delta}_r \psi_1 - ja_9 \check{\delta}_\mu \psi_1, \\ f_2 &= 1 + \varkappa_\rho - \frac{m}{\varepsilon_R} \beta_r - ja_6, \\ a_3^* &= (\mu^2 - 1)(1 + \beta_\mu)/\alpha = 1 - 1/a_3. \end{aligned}$$

Taking into account $\nabla\omega = -m\nabla\Omega$ we can easily obtain all the required derivations of the parameters.

Acknowledgements. The authors gratefully acknowledge financial support of the present work by the German Science Foundation (DFG) under grant No. 436 RUS 113/560/4-1.

References

- Abramowitz M., Stegun I.A. 1984, Pocketbook of Mathematical Functions. Verlag Harri Deutsch, Thun – Frankfurt/Main
- Bateman, H., Erdélyi, A. 1953, Higher Transcendental Functions. McGraw-Hill, New York
- Berthomieu, G., Gonczi, G., Graff, P., Provost, J., Rocca, A. 1978, A&A, 70, 597
- Bildsten, L., Ushomirsky, G., Cutler, C. 1996, ApJ, 460, 827
- Charbonneau, P., Tomczyk, S., Schou, J., Thompson, M. J. 1998, ApJ, 496, 1015
- Clement, M. J. 1998, ApJ, 116, 57
- Cox, J. P. 1980, Theory of Stellar Pulsation. Princeton Univ. Press, Princeton, USA
- Dzhililov, N. S., Staude, J., Oraevsky, V. N. 2001, A&A, (submitted)
- Dzhililov, N. S., Zhugzhda, Y. D. 1990, AZh, 67, 561
- Eckart, C. 1960, Hydrodynamics of Oceans and Atmospheres. Pergamon Press, Oxford, England
- Gill, A. E., 1982, Atmosphere-Ocean Dynamics. Acad. Press, Univ. of Cambridge, England
- Gilman, P. A., Fox, P. A. 1997, ApJ, 484, 439
- Heun, K. 1889, Math. Annalen, 33, 161
- Knobloch E., Spruit H. C. 1982, A&A, 113, 261
- Laplace, P. S. 1778-1779, Recherches sur Plusieurs Points du Système du Monde (extracts from Mémoires de L'Academie Royale des Science, 1775, 1776)
- Lee, U., Saio, H. 1986, MNRAS, 221, 365
- Lee, U., Saio, H. 1997, ApJ, 491, 839
- Ledoux, P. 1951, ApJ, 114, 373
- Lindzen, R. S., Chapman, S. 1969, Space Sc. Rev., 10, 3
- Oraevsky, V. N., Dzhililov, N. S. 1997, Astron. Rep., 41, 91
- Papaloizou, J., Pringle, J. 1978, MNRAS, 182, 423
- Pedlosky, J. 1982, Geophysical Fluid Dynamics. Springer-Verlag, New York-Heidelberg-Berlin
- Provost, J., Berthomieu, G., Rocca, A. 1981, A&A, 94, 126
- Rayleigh, J. W. S. Lord 1880, Proc. Lond. Math. Soc., 11, 57
- Saio, H. 1982, ApJ, 256, 717
- Smeyers, P., Craeynest, D., Martens, L. 1981, Astrophys. Space Sci., 78, 483
- Stix, M., Skaley, D. 1990, A&A, 232, 234
- Townsend, R. H. D. 1997, MNRAS, 284, 839
- Unno, W., Osaki, Y., Ando, H., Shibahashi, H. 1989, Nonradial Oscillations of Stars. Univ. of Tokio Press, Tokyo
- Watson, M. 1981, Geophys. Astrophys. Fluid Dyn., 16, 285
- Wolff, C. L. 1998, ApJ, 502, 961

Table .1. Results for the 22-year period: frequency deviations $\delta = \omega_{22} - \omega$ for permitted quantum numbers $(l, |m|)$

l	m	δ	m	δ	l	m	δ	m	δ	l	m	δ	m	δ
	fast	(nHz)	slow	(nHz)		fast	(nHz)	slow	(nHz)		fast	(nHz)	slow	(nHz)
11	1	0.055	575	0.000	33	10	-0.021	478	0.000	55	35	-0.008	365	-0.001
12	1	0.250	571	0.001	34	10	0.051	474	0.001	56	36	0.010	360	0.001
13	1	0.406	567	0.001	35	11	0.020	469	0.000	57	38	0.007	354	0.001
14	2	-0.265	562	-0.001	36	12	-0.003	464	0.000	58	40	0.007	348	0.001
15	2	-0.073	558	0.000	37	13	-0.021	459	-0.001	59	43	-0.008	341	-0.001
16	2	0.089	554	0.000	38	14	-0.033	454	-0.001	60	45	-0.004	335	0.000
17	2	0.226	550	0.001	39	14	0.029	450	0.001	61	47	0.002	329	0.000
18	3	-0.128	545	-0.001	40	15	0.020	445	0.001	62	50	-0.005	322	-0.001
19	3	0.013	541	0.000	41	16	0.014	440	0.001	63	52	0.004	316	0.001
20	3	0.136	537	0.001	42	17	0.012	435	0.000	64	55	0.001	309	0.000
21	4	-0.091	532	-0.001	43	18	0.012	430	0.000	65	58	0.002	302	0.000
22	4	0.028	528	0.000	44	19	0.014	425	0.001	66	61	0.004	295	0.001
23	4	0.134	524	0.001	45	20	0.018	420	0.001	67	65	-0.001	287	0.000
24	5	-0.021	519	0.000	46	22	-0.019	414	-0.001	68	69	-0.002	279	-0.001
25	5	0.079	515	0.001	47	23	-0.010	409	-0.001	69	73	-0.001	271	0.000
26	6	-0.035	510	0.000	48	24	0.001	404	0.000	70	77	0.002	263	0.000
27	6	0.058	506	0.001	49	25	0.011	399	0.001	71	82	0.001	254	0.000
28	7	-0.029	501	0.000	50	27	-0.009	393	-0.001	72	88	0.000	244	0.000
29	7	0.057	497	0.001	51	28	0.005	388	0.000	73	94	0.001	234	0.001
30	8	-0.009	492	0.000	52	30	-0.009	382	-0.001	74	102	0.000	222	0.000
31	9	-0.060	487	-0.001	53	31	0.006	377	0.001	75	112	-0.001	208	0.000
32	9	0.019	483	0.000	54	33	-0.002	371	0.000	76	125	0.000	191	0.000